RSC Advances

ROYAL SOCIETY OF CHEMISTRY

www.rsc.org/advances

In Situ Synthesis of Ultra-small Platinum Nanoparticles Using Water Soluble Polyphenolic Polymer with High Catalytic Activity

Tanmoy Maji, Sanjib Banerjee, Mrinmoy Biswas and Tarun K. Mandal*

Abstract: A simple and convenient strategy is described for the *in situ* synthesis of ultra-small platinum nanoparticles (Pt NPs) at room temperature using poly(4-vinyl phenol) (PVPh) as both the reducing as well as the stabilizing agent in aqueous alkaline solution. This strategy excludes the use of any additional stabilizing agent in addition to use a reducing agent. Transmission electron microscopic analysis confirms the formation of ultra-small spherical Pt NPs from 1.6 ± 0.2 to 2.2 ±0.2 nm in diameter with a high degree of monodispersity depending on ratio of PVPh to platinum salt concentrations used in a single reaction. The as-synthesized ultra-small Pt NPs exhibits extremely high catalytic activity towards the borohydride reduction of p-nitrophenol with very low activation energy (E_a = 24.6 kJ mol^{-1}). Furthermore, the ultra-small PVPh-capped Pt NPs are successfully used as an excellent catalyst for hydrogenations of styrene and nitrobenzene in methanol with very high yield. The PVPh-capped Pt NPs are reusable up to four cycles of catalysis reaction, although there is a substantial loss of its original activity after the first cycle.

*Polymer Science Unit, Indian Association for the Cultivation of Science, Jadavpur, Kolkata 700 032, India. E-mail: psutkm@iacs.res.in; Fax: (+91) 33-2473-2805.

1. Introduction

Transition metal nanoparticles (NPs) such as gold (Au), platinum (Pt) have received great attention in the field of nanoscience and other interdisciplinary areas of the scientific research due to their interesting optical, electronic, and catalytic properties.[1, 2] Among these transition metal NPs, the significance of Pt NPs is going up day by day. The uprising interest in Pt NPs is not only due to its well-established catalytic properties, but also due to its extensive potential use in biomedical, electronic devices[3] and recently as catalyst in electrochemical reactions of fuel cells.[4] Again all of these applications require Pt NPs of well-defined size, size distributions and morphologies.[5-8] Studies revealed that the size of Pt NPs (especially <5 nm) impart an obvious effect on its catalytic activity and selectivity due to larger numbers of surface atoms available for catalysis shifting the Fermi level more in presence of highly electron injecting species like BH_4^- ions.[9-13] Thus, the synthesis of highly active ultra-small Pt NPs of controlled morphologies is of great importance.

Several research groups have reported syntheses of small sized Pt NPs by different methods such as using polyols including ethylene glycol, ethanol or short chain polyethylene glycol,[14-16] borohydride and/or hydrogen or methods like electrochemical deposition,[17, 18] physical vapour deposition[19] or light-driven synthesis.[20] Xia et al. reported synthesis of ~5 nm range Pt NPs by polyol reduction method in presence of poly(vinyl pyrrolidone) (PVP) as stabilizer at a temperature of 110 °C.[15] Luong et al. prepared small sized (2.5 ± 0.7 nm) Pt NPs using sodium citrate both as reducing agent and as colloid stabilizer at 80 °C.[21] However, for synthesising such ultra-small Pt NPs in colloidal/wet chemical methods higher temperature is required.[22, 23] There are also few reports of synthesis of Pt NPs at lower temperature.[24-27] Huang et al. have reported synthesis of ultra-small Pt nanocrystals by boryhydride reduction method using peptide as stabilizer at room temperature.[6] El-Sayed et al. produced Pt NPs of size <5 nm stabilized by PVP by hydrogen reduction method.[28]

However, to the best of our knowledge, there is no report of synthesis of ultra-small Pt NPs by a polymeric reducing agent which also can act as the stabilizer at ambient temperatures.

It is well known that noble metals nanoparticles such as Pd, Au, and Pt are promising catalysts for various organic and inorganic reactions.[23, 26, 29] Among them, Pt NPs possesses very high catalytic activity and stability for which it is used in many technological applications.[30, 31] Catalytic efficiency and selectivity of NPs are highly dependent on the size and shape of the nanomaterials. To study the catalytic activity of Pt NPs towards borohydride reduction of 4-nitrophenol to 4-aminophenol is taken as a model reaction by number of research groups[32, 33] where it exhibits excellent catalytic efficiency. Pt NPs can reduce the activation energy of this catalysis reaction even up to 18.5 kJ mol^{-1} but those only for the case of surface catalyzed reaction.[33] However, there exists no report of colloidal Pt NPs with activation energy < 25 kJ mol^{-1} for borohydride reduction of 4-nitrophenol to 4-aminophenol.

Thus, in this work, we report a simple and convenient strategy to synthesize ultra-small (< 2 nm) Pt NPs using only alkaline poly 4-vinylphenol (PVPh) solution at room temperature. Earlier, our group has reported synthesis of water-dispersible Au NPs by an in situ redox technique at room temperature using PVPh as a simultaneous template/stabilizer and reducing agent.[34] The size of the Au NPs were relatively large and polydisperse in size (6-13 nm). In this work, we report the formation of nearly monodisperse ultra-small (< 2 nm) spherical Pt NPs as observed via transmission electron microscopy (TEM). Thermo-gravimetric analysis (TGA) is performed to confirm the presence of PVPh on the surface of the synthesized Pt NPs. Additionally, to evaluate the catalytic activity of the nearly monodipersed colloidal ultra-small Pt NPs, borohydride reduction of 4-nitrophenol to 4-aminophenol is taken as a model reaction.

2. Experimental

2.1 Materials

Poly(4-vinyl phenol) (PVPh) (Aldrich), hydrogen hexachloroplatinate (IV) hydrate ($H_2PtCl_6.xH_2O$) (Aldrich, purity >99.9%), NaOH (Merck, India), sodium borohydride ($NaBH_4$) (Spectrochem, India), 4-nitrophenol (4-$C_6H_5NO_3$, 4NP) (Spectrochem, India), nitrobenzene (Spectrochem, India) were used as received. Styrene (Aldrich, purity >99.9%) passed through a column filled with basic aluminum oxide and methanol (MeOH) (Merck, India) was distilled prior to use. Glass apparatus and cover slides were purchased from Blue Star, India Ltd. and were cleaned with aqua-regia solution and then rinsed thoroughly with double distilled water prior to use. All of the aqueous solutions were made with Milli-Q water.

2.2 Synthesis of ultra-small platinum (Pt) nanoparticles (NPs) using PVPh

Pt NPs of varying sizes were prepared by the reduction of an appropriate mixture of the precursor salt, $H_2PtCl_6.xH_2O$ using alkaline PVPh in water. In a typical synthesis, 1.2 mL of alkaline (pH≈12) PVPh solution (0.8 wt %,) and 5.78 mL Milli-Q water were taken in a borosil culture tube maintained at room temperature with constant magnetic stirring. To this stirring solution, 1.04 mL of 10 mM H_2PtCl_6 was added. The pH of the final mixture was maintained at pH 11. The reaction mixture was then magnetically stirred at room temperature for a weak. Two different samples PVPh-$Pt_{1.3}$, PVPh-Pt_5 were synthesised maintaining 1.3 mM and 5 mM H_2PtCl_6 concentration (see Table 1) in the reaction mixture.

2.3 Synthesis of Pt NPs without PVPh using $NaBH_4$ (Bare-Pt NPs)

Bare-Pt NPs were also prepared by simple stirring of 4 mL of aqueous H_2PtCl_6 (5 mM) solution at room temperature with solid $NaBH_4$ (8 mg, 0.212 mmol) for 10 min (see Table 1). After centrifugation at 8000 rpm the upper aqueous part was decant and black Pt NPs were isolated and vacuum dried at 70 °C for 24 h.

Table 1. Reaction recipe for the synthesis of Pt NPs and their characterizations.

Sample	[PVPh] (wt%)	[$NaBH_4$] (mM)	[H_2PtCl_6] (mM)	*Shape*	D_{TEM} (nm)
PVPh-$Pt_{1.3}$	0.12	0	1.3	Spherical and nonaggregated	2.2 ± 0.2
PVPh-Pt_5	0.12	0	5.0	Spherical and nonaggregated	1.6 ± 0.2
PVPh-Pt_{BH4}^-	0.12	18.3	1.3	Spherical and aggregated	~2.8
Bare-Pt	0	53	5.0	Spherical and aggregated	~3.5

2.4 Synthesis of colloidal PVPh stabilized Pt NPs using $NaBH_4$ (PVPh-Pt_{BH4^-})

An alkaline (pH≈12) PVPh solution (1.2 mL, 0.8 wt %,) and 5.76 mL Milli-Q water were taken in a borosil culture tube maintained at room temperature with constant magnetic stirring. To this stirring solution, 1 mL of 10 mM H_2PtCl_6 was added followed by drop wise addition of 0.60 mL $NaBH_4$ solution (0.1 wt %) at 25 °C which was then used for further reaction.

2.5 Study of catalytic activities of Pt NPs on borohydride reduction of 4-nitrophenol

This reaction has been used as model reaction to study the catalytic activities of several metal nanoparticles by many researchers including our group.[33, 35-39] Typically, in this case, for the catalytic activity study, a stock aqueous suspension was first prepared by dilution of 0.5 mL as-synthesised colloidal Pt NPs suspension (PVPh-$Pt_{1.3}$) to 2.5 mL with Milli-Q water. The catalytic reaction was then performed by taking an aliquot of 2 mL of the above stock solution which contained 0.1 mg Pt nanocatalyst, 0.8 mL water, and an aqueous 4-NP solution (0.1 mL, 3 mM), into a 3 mL quartz cuvette under stirring of 500 rpm in a

spectrophotometer at 25 °C. To this reaction mixture, an aqueous $NaBH_4$ solution (0.1 mL; 300 mM) was finally added to study the reduction of 4-NP. The same reaction was performed at 25, 30 and 40 °C to determine the activation energy of the as-synthesised Pt NPs. For comparison, we also carried out borohydide reduction of 4-NP with the colloidal Bare-Pt NPs and borohydride reduced PVPh-stabilized Pt NPs (PVPh-Pt_{BH4}^-) (see Electronic supplementary information for experimental details).

2.6 Catalysis of hydrogenation reaction in organic medium

One of the important reactions in chemistry catalysed by metallic platinum is the hydrogenation reaction. Hence, we explored the catalytic activity of PVPh-Pt_5 as a typical sample toward hydrogenation of styrene and also nitrobenzene as specific substrates. The as synthesised colloidal Pt nanocatalyst (PVPh-Pt_5) was first precipitated from water reducing the pH to 5 and then freeze-dried. The obtained solid PVPh-Pt nanocatalyst composite was then used for hydrogenation reaction. For hydrogenation reaction, 1.3 mg of PVPh-Pt_5 (38.2 wt % Pt NPs) catalyst was dispersed in 1.5 mL MeOH followed by addition of 0.15 mL of styrene (1.30 mmol) or 0.15 mL of nitrobenzene (1.46 mmol) under nitrogen atmosphere. The mole ratio of substrate:Pt NPs was > 500:1. Finally the reaction mixture was vigorously stirred for 3h under hydrogen atmosphere (1 atm) at 25 °C. After the reaction the solution mixture was concentrated and added excess chloroform. The precipitated PVPh polymer along with Pt NPs was separated from product by centrifugation at 8,000 rpm for 5 min. The organic solvents were then evaporated to get the hydrogenated product. The product was characterized by NMR spectroscopy and gas chromatography-mass spectrometry (GC-MS) which showed that we obtained more or less pure product by this procedure.

2.7 Reusability of PVPh-capped Pt NPs in the borohydride reduction of 4-NP

The synthesised ultra-small Pt NPs can be easily isolated by decreasing the pH of the solution to 5 and also can be dispersed in water and can be utilised for further catalysis reaction.

Hence, we examined reusability of a representative catalyst PVPh-$Pt_{1.3}$. For this, we first performed the catalysis of borohydride reduction of 4-NP by the same procedure as mentioned above. After the reaction the PVPh-$Pt_{1.3}$ catalyst was centrifuged out from the solution at a pH ~5 and washed thoroughly with acidic water of pH~5 and then redispersed in aqueous alkaline solution of pH 8 for the next catalysis cycle.

2.8 Characterization

UV-vis absorption spectroscopy. To study the progress of the reaction of formation of Pt NPs, 1.0 mL reaction mixture was taken out at a predetermined intervals and UV-vis spectrum was recorded using a Hewlett Packard 8453 diode array spetcrophotomer. The catalytic activities of Pt NPs in the borohydride reduction of 4-NP were studied in a 1 cm path length quartz cuvette via the spectral analysis using a Hewlett-Packard 8453 diode-array spectrophotometer.

Transmission Electron Microscopy (TEM). For TEM study, a drop of the Pt NPs sample's aqueous suspension was casted onto a carbon-coated copper grid and dried at room temperature for 24 h and imaged at an accelerating voltage of 200 kV under a JEOL high-resolution electron microscope (model JEM 2010E). HRTEM image and energy-dispersive X-ray (EDX) spectrum was also acquired for each sample.

Dynamic light scattering (DLS). All DLS experiments of colloidal Pt NPs' suspension were carried out at 25 °C on a Malvern Particle Size Analyzer (Model No. ZEN 3690 Zetasizer NANO ZS90).

Thermogravimetric analysis (TGA): For TGA analysis, the samples were precipitated by decreasing the pH at 2 and then air dried overnight followed by vacuum dried at 70 °C for 24 h. Bare-Pt NPs and neat PVPh were vacuum dried at the same condition before analysis. All the samples were then analysed in TA (SDT Q600) thermal analyser instrument at a heating rate of 20 °C min^{-1} under nitrogen atmosphere.

Gas chromatography-mass spectrometry (GC-MS): GC-MS measurements of the obtained organic products after catalysis were carried out on a PerkinElmer Clarus 680 GC with an attachment Clarus SQ8T mass spectrometer using Elite 5 MS (30 m x 0.25 mm x 0.25 μm) column with maximum temperature of 300 °C.

NMR spectroscopy: All the ^{1}HNMR and ^{13}C NMR spectra of organic compounds were recorded on a Bruker Avance 500 MHz spectrometer $CDCl_3$ as the solvent and TMS as the internal reference.

3. Results and Discussion

Two different types of Pt NPs samples were prepared by varying the concentration of Pt salts and keeping the PVPh concentration constant (pH~11) in water at room temperature (see experimental section for details). The reaction conditions and the detailed recipes for the synthesis of Pt NPs samples were given in Table 1. It is reported that PVPh is soluble in alkaline water and its phenolate group can stabilise metal nanoparticles.[40] The phenolate group is also able to reduce metal salts into their corresponding nanoparticles.[41, 42] Thus, we have chosen PVPh as a stabilizer-cum-reducing agent for this *in situ* Pt NPs synthesis from H_2PtCl_6.

Figure 1 showed the UV–vis absorption spectra of the aqueous solution of PVPh and H_2PtCl_6 reaction mixture under the same experimental condition but at different time without any further purification. It was observed that there was a broad absorption peak at around 262–265 nm, which is assigned to the ligand-to-metal ($Cl^- \rightarrow Pt^{4+}$) charge transfer transition of $[PtCl_6]^{2-}$ ions.[32] Figure 1 also revealed that with the increase of reaction time, absorbance in this range decreases. This indicates the reduction of H_2PtCl_6 by only reducing agent present in the reaction mixture, phenolate group of PVPh, which in turn suggests the formation of Pt NPs in the reaction mixture.

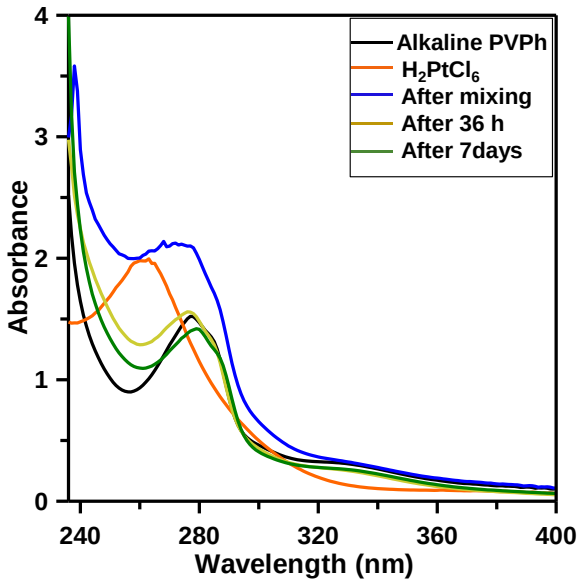

Figure 1. UV-Vis spectra of alkaline PVPh, aqueous H_2PtCl_6 and reaction mixtures taken at different time intervals during the synthesis of PVPh-$Pt_{1.3}$ sample.

To visualize the size and shape of the *in situ* formed Pt NPs, aliquots were taken out of the reaction mixture and examined via TEM (Figure 2). TEM images of PVPh-$Pt_{1.3}$ and PVPh-Pt_5 (see Figure 2A and 2B respectively) clearly showed formation of highly dispersed ultra-small spherical Pt nanostructures. Inset of Figure 2A and 2B shows the histogram of particle size distributions of the corresponding samples which clearly revealed the formation nearly uniformly dispersed Pt NPs. Notably, PVPh-Pt_5 have narrow size distribution of average diameter of 1.6 ± 0.2 nm than that of PVPh-$Pt_{1.3}$ sample having average diameter 2.2 ± 0.2 nm. Also, no aggregated Pt NPs was observed in the TEM image. The as synthesized PVPh capped Pt NPs are very small in size and are highly dispersed in solution. As mentioned above, an alkaline PVPh solution was used as reducing agent for conversion of H_2PtCl_6 to Pt NPs. Alkaline PVPh have low reduction potential and can also act as stabilizer. Hence, polyphenolic PVPh stabilizer restrict the growth of initially formed Pt nuclei and as a result highly dispersed ultra-small Pt NPs are produced in an optimum reaction condition.[43]

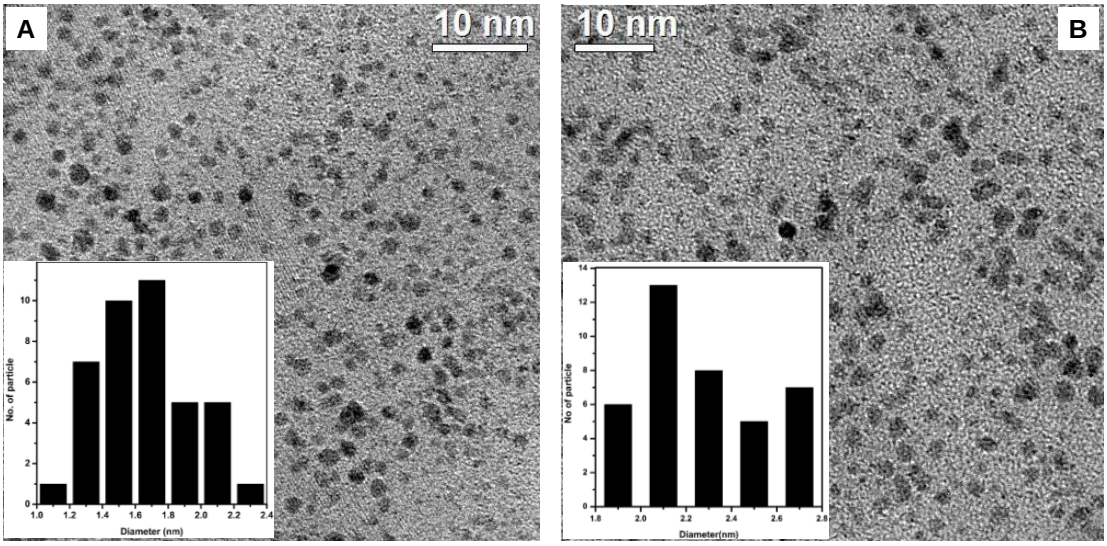

Figure 2. TEM images of (A) PVPh-Pt_5 (B) PVPh-$Pt_{1.3}$ samples. Inset in each panel showed the histogram of particle size distribution of Pt NPs.

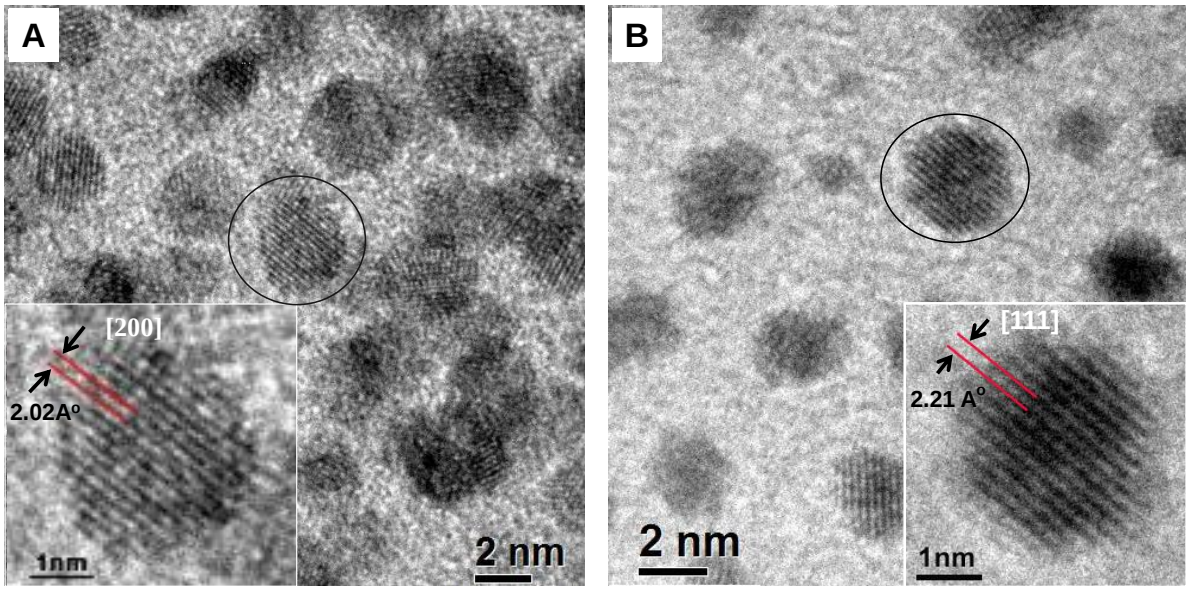

Figure 3. TEM images of (A) PVPh-$Pt_{1.3}$ (B) PVPh-Pt_5. Insets in each panel showed the HRTEM of single particle.

The magnified images of samples PVPh-$Pt_{1.3}$ and PVPh-Pt_5 were given in Figure 3A and 3B respectively. Inset of Figure 3A and 3B presented the HRTEM image of single Pt NP (circled) of the corresponding sample showing aligned lattice fringes with an interplanar spacing of 2.21 *Aº* and 2.02 *Aº* corresponding to the [111] and [200] planes of platinum face

centred cubic structure[44] (JCPDS No. 04-0802). HRTEM images of colloidal Bare-Pt NPs and colloidal borohydride reduced PVPh stabilized Pt NPs (PVPh-Pt_{BH4^-}) (Figure S1 in the ESI) were also acquired to compare with PVPh-$Pt_{1.3}$ and PVPh-Pt_5 NPs samples. As can be seen that both the samples (Bare-Pt and PVPh-Pt_{BH4^-}) showed an aggregated structure throughout the TEM grid which was composed of small nanosized particles (~3.5 nm of Bare-Pt NPs and ~2.8 nm of PVPh-Pt_{BH4^-}). Energy dispersive X-ray (EDX) measurements of each sample gave further evidence of presence of Pt in the sample (Figure S2 in the ESI).

Hydrodynamic diameters of the as-synthesised Pt NPs measured from DLS were 11.4 and 11.70 nm for PVPh-Pt_5 and PVPh-$Pt_{1.3}$ samples respectively (Figures S3-S4 in the ESI). DLS analysis also revealed the formation of nearly monodisperse Pt NPs.

The anchoring of PVPh on the surface of Pt NPs and conversion of H_2PtCl_6 to nanoparticle was confirmed from TGA of the purified and dried samples. The TGA thermograms of Pt NPs samples were shown in Figure 4 along with the TGA thermogram of neat PVPh and bare-Pt NPs for comparison. Thermograms of the PVPh-Pt nanocomposites showed a significant weight loss in the temperature range from 120 °C to 700 °C. This weight loss is due to PVPh only because the metal NPs remains thermally stable at that temperature range. Assuming complete decomposition of PVPh at 700 °C, TGA thermogram revealed the presence of 13.3% and 38.2% of metallic Pt in PVPh-$Pt_{1.3}$, PVPh-Pt_5 samples where the theoretical feed ratio were 17% and 44% for those samples respectively. The TGA thermogram of PVPh-Pt_5 showed that the material was stable only up to ~210 °C, whereas neat PVPh was stable up to ~340 °C. This indicates that the Pt NPs promotes the decomposition of PVPh, which further signify the absorption of PVPh on the surface of Pt NPs.

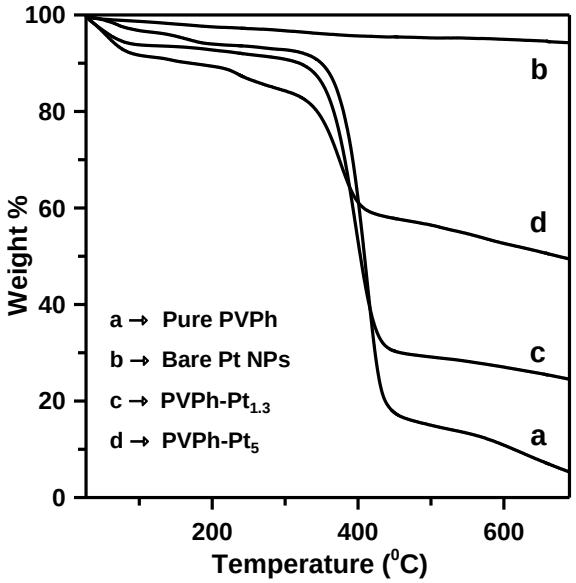

Figure 4. TGA thermograms of (a) neat PVPh, (b) Bare-Pt NPs, (c) PVPh-$Pt_{1.3}$ and (d) PVPh-Pt_5.

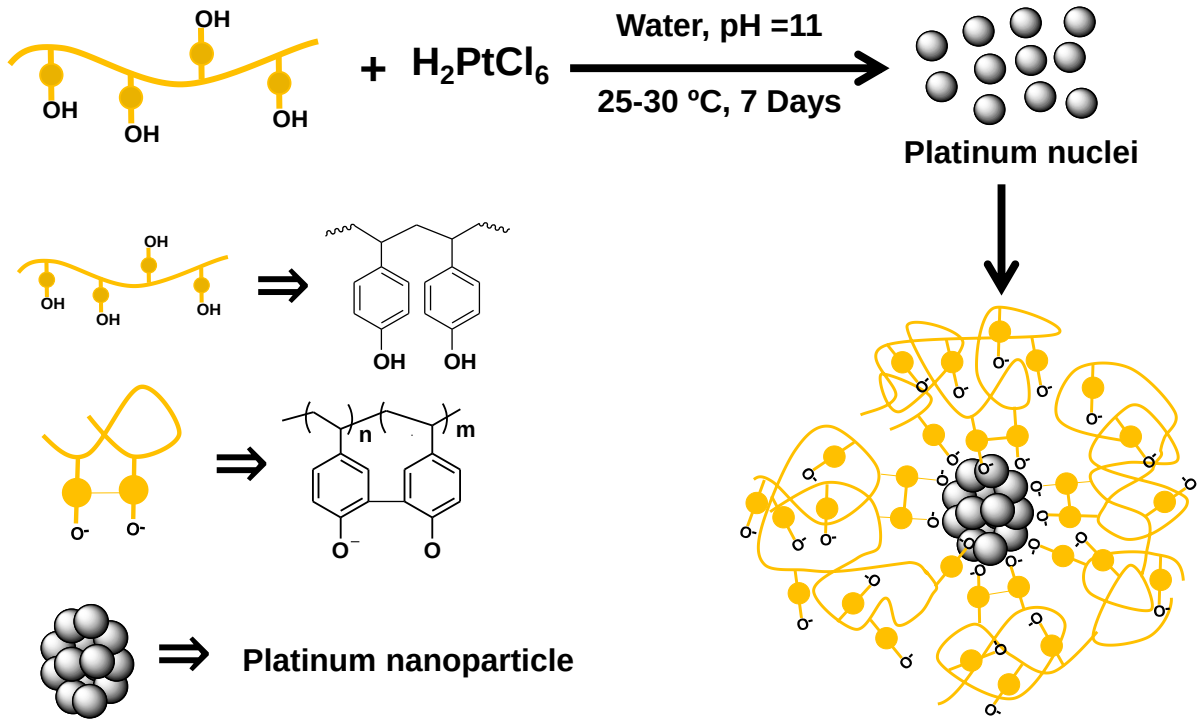

Scheme 1. Proposed mechanism for the formation of ultra-small Pt NPs.

From the above results, it was observed that the PVPh molecule is responsible for both reduction of H_2PtCl_6 to metallic Pt and the stabilization of the formed Pt NPs through its adsorption on Pt surface. Herein, we propose the formation mechanism of ultra-small PVPh capped Pt NPs as shown in Scheme 1. The phenolate groups of PVPh reduced H_2PtCl_6 to metallic Pt, which eventually combine to form Pt nuclei. There is an equilibrium between the Pt nuclei formation and the adsorption of PVPh through the functional phenolate groups resulting a polymer coating on the surface of the formed Pt NPs.[45] The coating of PVPh prevents Pt NPs from particles coalescence and slows down monomer attachment onto the NP surface excellently resulting in the formation of ultra-small Pt NPs.[46]

In order to study the catalytic activity of the as-formed ultra-small Pt NPs, the reduction of 4-nitrophenol (4-NP) to 4-aminophenol (4-AP) was chosen as a model reaction (see Scheme 2) as investigated by many groups including our group for various other metal NPs.[32, 47, 48] The mechanism of reduction of 4-NP to 4-aminophenol by $NaBH_4$ in the presence of Pt NPs is well documented in the literature by many research groups using the Langmuir-Hinshelwood (LH) model.[49, 50] The borohydride first adsorbs on the nanoparticles surface with the formation of metal hydride. Concomitantly, 4-NP adsorbs onto the metal surface. Then the reduction occurs in the rate determining step. Although this reaction is a thermodynamically feasible process, it is kinetically restricted in the absence of a catalyst.[47]

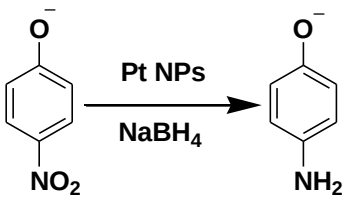

Scheme 2. The brohydride reduction of 4-nitrophenol (4-NP) to 4-aminophenol (4-AP).

In the presence of catalysts, such as noble metal NPs, like Au,[48] Ag[36] and Pt[33] the reaction takes place rapidly. Interestingly, the progress of this reaction can be monitored conveniently using UV-vis absorption spectroscopy. Figure 5 showed the time-dependent absorption spectra taken during the reduction of aqueous 4-NP by $NaBH_4$ at 25 °C in the presence of as-synthesised PVPh-capped Pt NPs samples. The absorption spectra of catalytic reaction

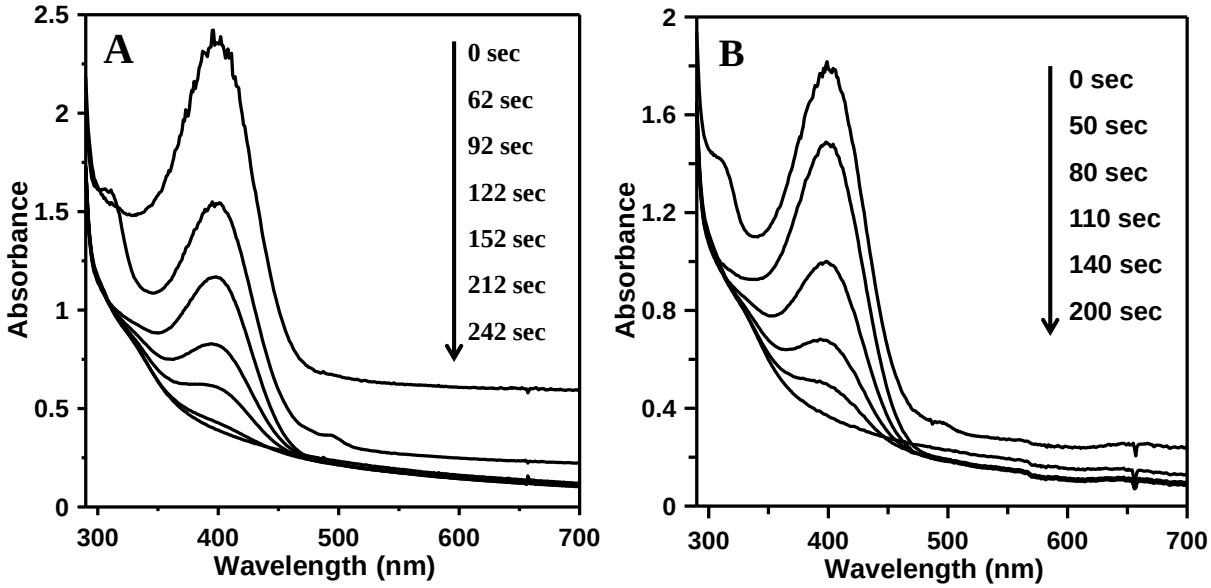

Figure 5. Time-dependent absorption spectra of the 4-NP reduction in the presence of (A) PVPh-$Pt_{1.3}$ (B) PVPh-Pt_5 samples at 25 °C

mixture taken at 30 °C and 40 °C were given in Figure S5 and Figure S6 respectively in the ESI. A rapid decrease of the peak intensity at λ = 400 nm corresponding to the 4-nitrophenolate anion indicates the reduction of 4-NP.[36, 51] In general a peak at 300 nm due to 4-aminophenol appears with concomitant disappearance of peak at 400 nm of 4-nitrophenol during the kinetic study of 4-nitrophenol reduction via UV-vis spectroscopy. But, in this case, the growing peak at 300 nm was hardly noticed. This is because of the overlapping of this 4-AP peak (300 nm) with the absorption peak (at 280 nm, see Figure 1) due to π-π^* transition of phenol moiety of polyphenolic polymer attached with the Pt catalyst, in this particular

range. However, we observed this 4-AP peak (300 nm) when Bare-Pt NPs was used for the reduction of 4-nitrophenol as there is no PVPh attached with Pt surface (see Figure S7A).

The concentration of $NaBH_4$ in the reaction mixture was much excess than that of 4-NP and for this it can be regarded as being constant throughout the reaction. Hence, the reaction can be treated as a pseudo first order reaction. The apparent rate constant (k_{app}) at different temperatures of this catalytic reaction for PVPh-caped Pt NPs samples were

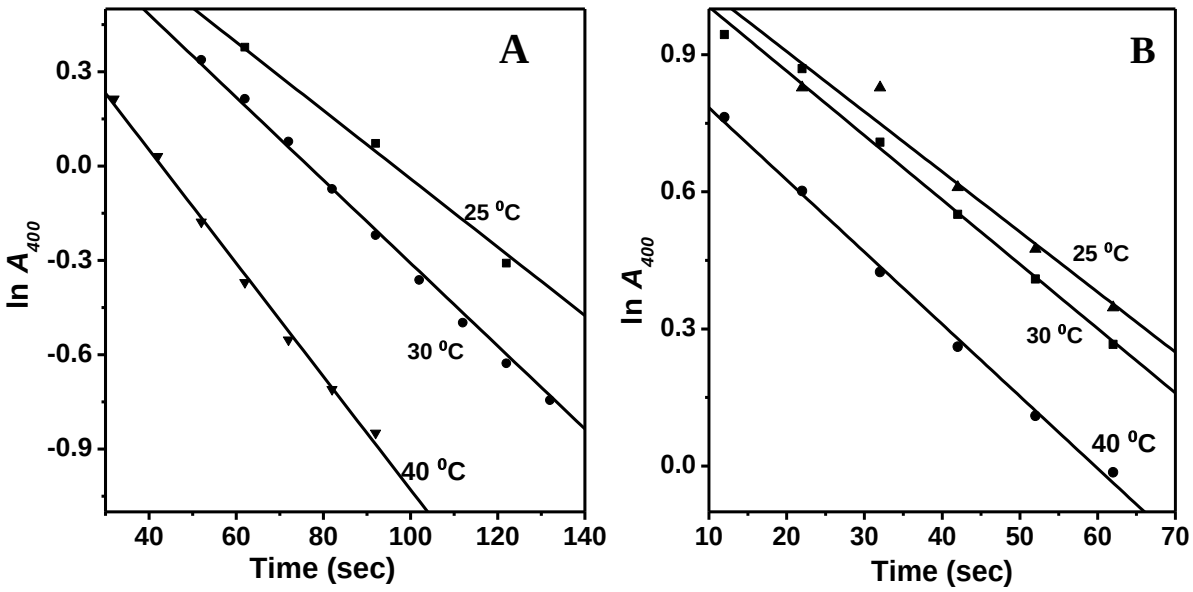

Figure 6. Plots of ln A (A = absorbance at 400 nm of p-nitrophenolate ion) versus time for the reduction of p-nitrophenol sample at three different temperatures using (A) PVPh-$Pt_{1.3}$ (B) PVPh-Pt_5.

calculated from the slope of the plots given in Figure 6. For instance, the k_{app} of this catalytic reaction evaluated from the slope of the plot of lnA_{400} versus time (Figure 6A) at 30 °C was 0.01318 s^{-1} for 5.1×10^{-4} mmol of sample PVPh-$Pt_{1.3}$ (assuming complete conversion of H_2PtCl_6). Thus, the normalized rate constant (k_{nor}) of this catalytic reaction was calculated to be 25.84 s^{-1} $mmol^{-1}$ for PVPh-$Pt_{1.3}$ at this temperature. The k_{app} and k_{nor} values at other temperatures were also obtained by the same procedure for the PVPh-$Pt_{1.3}$ and PVPh-Pt_5

samples and were given in Table 2 and Table 3. We found that the k_{nor} was much higher than that of previously reported values for Ag[36], Au[52] and also for Pt[33] NPs at 30 °C due to pseudo homogenous nature of the catalyst. In general, pseudo homogeneous catalysis favors, where the respective nanocatalyst is very small in size and is highly dispersed. A decrease in the nanoparticle size increases the surface area or surface area to volume ratio which provides a higher diffusion of substrates like 4-NP to the nanoparticles' surface and eventually increase the catalytic reaction rate. Therefore, the above mentioned PVPh-Pt NPs catalyst has superior catalytic activity compare to that reported for other mental nanoparticles.

Table 2. Catalytic rate constants of the borohydride reduction of 4-NP in the presence of the PVPh-$Pt_{1.3}$ sample.

Temperature (^{0}C)	**Amount (mmol)**	k_{app} **(s^{-1})**	k_{nor} **(s^{-1} $mmol^{-1}$)**
25	5.1×10^{-4}	1.08×10^{-2}	21.31
30	5.1×10^{-4}	1.32×10^{-2}	25.84
40	5.1×10^{-4}	1.09×10^{-2}	35.33

Table 3. Catalytic rate constants of the borohydride reduction of 4-NP in the presence of the PVPh-Pt_5 sample.

Temperature (^{0}C)	**Amount (mmol)**	k_{app} **(s^{-1})**	k_{nor} **(s^{-1} $mmol^{-1}$)**
25	2.0×10^{-3}	1.12×10^{-2}	5.62
30	2.0×10^{-3}	1.38×10^{-2}	6.91
40	2.0×10^{-3}	1.86×10^{-2}	9.31

For comparison, we have done this catalytic reaction with colloidal Bare-Pt NPs and PVPh-Pt_{BH4^-} NPs. The time dependent absorption spectra of colloidal Bare-Pt NPs and PVPh-Pt_{BH4^-} were given in Figure S7 in the ESI. The rate constants were then determined

from the slope of the plots given in Figure S8 of the ESI and were given in Table 4 for colloidal Bare-Pt NPs and PVPh-Pt_{BH4^-}. It should be noted that the *in situ* synthesised ultra-small PVPh capped Pt NPs (PVPh-$Pt_{1.3}$) exhibited much higher catalytic activity at 25 °C than those of Bare-Pt NPs and PVPh-Pt_{BH4^-} samples with aggregated structure.

Table 4. Catalytic rate constants of the borohydride reduction of 4-NP in the presence of the synthesised Pt NPs catalyst

Sample	Amount (mmol)	k_{app} (s^{-1})	k_{nor} (s^{-1} $mmol^{-1}$)
Bare Pt NPs	5.7×10^{-4}	1.51×10^{-3}	2.65
PVPh-Pt_{BH4^-}	5.1×10^{-4}	2.1×10^{-3}	4.12
PVPh-$Pt_{1.3}$	5.1×10^{-4}	1.08×10^{-2}	21.18

The activation energies of this catalytic reaction for PVPh-$Pt_{1.3}$ and PVPh-Pt_5 samples were calculated from the slope of the plot ln k_{nor} vs 1000/T (Figure 7A and Figure 7B). The

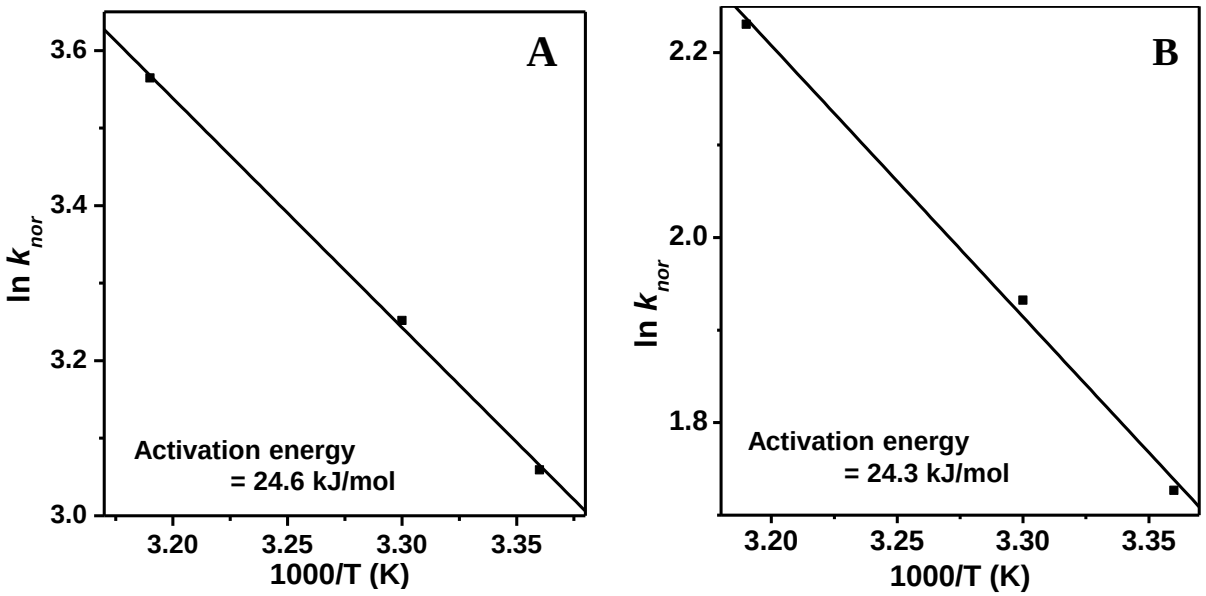

Figure 7. Plot showing the variation of ln k_{nor} with 1000/T for this catalytic borohydride reduction reaction using (A) PVPh-$Pt_{1.3}$ (B) PVPh-Pt_5.

calculated values of activation energies were found to be 24.6 kJ mol^{-1} and 24.3 kJ mol^{-1}. It should be noted these values are almost the same as the particle size of samples PVPh-$Pt_{1.3}$ PVPh-Pt_5 are very close. These values were also low compared to the reported values for the same reaction using PVP-caped cubic dominated Pt NPs (26.4 ± 1.2 kJ mol^{-1}),[53] citrate-stabilized Au nanoparticles (31 kJ mol^{-1}),[13] Ag nanoparticle-doped polymer film (40.9 kJ mol^{-1}) ,[54] Au/PMMA composite (38 kJ mol^{-1}).[55] Thus, we can conclude that ultra-small PVPh-capped Pt NPs is a promising nanocatalyst.

The hydrogenation reactions of olefins or carbonyl or nitro group using heterogeneous Pt nanocatalyst are very common.[56, 57] Thus, we choose these reactions to study the catalytic activities of these ultra-small Pt NPs in organic solvents. As the PVPh-capped Pt NPs are highly dispersiable in methanol, we choose this solvent for hydrogenation of styrene and nitrobenzene with a representative nanocatalyst, PVPh-Pt_5 (Scheme 3). The ^{1}HNMR and ^{13}CNMR spectra confirmed the formation of ethyl benzene and aniline (Figures S9- S12 in the ESI). The GC-MS spectra (Figures S13-S14 in the ESI) of the reaction products were acquired only after the removal of the Pt nanocatlyst by precipitation in chloroform followed by evaporation of solvents. We observed more than 99% conversion (measured by GC-MS) of styrene and nitrobenzene to ethyl benzene and aniline respectively in 3 h only in the presence of 1 atmospheric H_2 pressure at 25 °C.

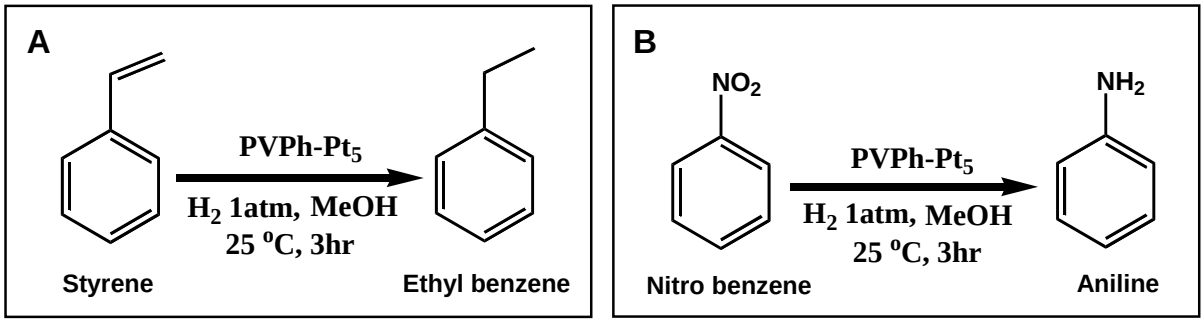

Scheme 3. Hydrogenation of (A) styrene into ethyl benzene and (B) nitrobenzene into aniline in MeOH at 25 °C using PVPh-Pt_5 sample.

The recycling and recovery of used catalysts, one of the important properties of metal catalysts. To check the reusability of the PVPh-capped ultra-small Pt NPs, a representative sample PVPh-$Pt_{1.3}$ was utilised for borohydride reduction of 4-NP. The catalyst sample PVPh-$Pt_{1.3}$ was recovered after first cycle of catalysis by decreasing the pH of the mixture to 5 and then centrifuged at 10,000 rpm for 5 min as the capping agent PVPh was insoluble at this pH. Then the catalyst was washed with water of pH~5. The catalyst was then redispersed in water at pH=8 in which the polymer is soluble and make the catalyst homogeneous again and used for the next catalyst cycle. By the similar procedure, borohydride reduction of 4-NP with the same catalyst was performed 4 times as a whole. The apparent rate constants were measured by the similar procedure as mentioned above from Figure S15 and Figure S16 in the ESI. Although there may be a chance of weight loss of the catalyst in recovering process, but the chances is very less. Hence, the normalized rate constants were calculated by considering 0% weight loss in each cycle and was plotted as a bar diagram in Figure S17 in the ESI. It was clear from Figure S17 that the activity of PVPh-capped Pt NPs catalyst decreased abruptly with respect to its original activity, which may be due to aggregation of the nanocatalyst after the cycle as observed from its TEM image (Figure S18 in the ESI). But still it can be reused as it showed 27% of its original activity after 4^{th} cycle. But, we observed a complete conversion of 4-NP to 4-AP in 13 min.

4. Conclusions

We have developed a simple water soluble polymer-based methodology for the synthesis of ultra-small nearly monodisperse spherical Pt NPs at ambient temperature by the reduction of Pt salt using PVPh as both reducing as well as stabilizing agent in aqueous alkaline solution. Formation of ultra-small nearly monodisperse Pt NPs was confirmed by HRTEM analysis and the associated particle size histogram. TGA analysis proved the binding of PVPh on the

surface of Pt NPs. PVPh reduced Pt^{4+} to Pt(0) and stabilized the formed Pt NPs through phenolate group, which regulated the nanoparticles nucleation and growth and, therefore, control both the morphology, size and size distribution of the Pt NPs. Uniform near spherical Pt NPs with a size from 1.6 to 2.4 nm were achieved with a narrow size distribution. Again these ultra-small Pt NPs showed very high catalytic activity towards the reduction of 4-nitrophenol to 4- aminophenol by $NaBH_4$. These ultra-small PVPh-capped Pt NPs can be used as an efficient catalyst for hydrogenations of styrene and nitrobenzene. The PVPh-capped Pt nanocatalyst can be reused up to four cycles, although there was a substantial loss of its original activity after first cycle.

Acknowledgement

T.M. thanks Council of Scientific & Industrial Research, India for fellowship. This research is supported by grants from the CSIR, New Delhi, India. Thanks are also due to the partial financial support from BRNS, India. We are also thankful to Prof. Dipak Khastgir (Rubber Technology Centre, IIT Kharagpur, India) for his kind support.

Electronic Supplementary Information (ESI) available: Procedure for catalysis of borohydride reduction of 4-NP with colloidal Bare-Pt NPs and colloidal PVPh-Pt_{BH4^-}, TEM images of colloidal Bare-Pt NPs and borhydride reduced PVPh-capped Pt NPs, Energy dispersive X-ray (EDX) spectra of PVPh-capped Pt NPs, DLS data of colloidal Pt NPs, time-dependent absorption spectra of the 4-NP reduction in the presence of PVPh-Pt nanoparticles' samples at 30 ºC and 40 ºC, 4-NP reduction at 25 °C in the presence of Bare- Pt and PVPh-Pt_{BH4^-} NPs, plots of ln A versus time for the reduction of 4-NP sample at 25 °C using catalyst 1. PVPh-$Pt_{1.3}$ 2. PVPh-Pt_{BH4^-} 3. colloidal Bare-Pt NPs, ^{1}HNMR, ^{13}C NMR and GC-MS spectra of ethyl benzene and aniline, time-dependent absorption spectra for reusable cycle of

4-NP reduction in the presence of PVPh-Pt NPs, plots of ln A versus time for the reduction of 4-NP for reusable cycle at 25 ºC, plot showing the variation in normalized rate constant in different cycles for 4-NP reduction, TEM image of PVPh-Pt NPs after catalysis. This material is available free of charge via the Internet at http://pubs.rsc.org.

Notes and References

1. S. Mostafa, F. Behafarid, J. R. Croy, L. K. Ono, L. Li, J. C. Yang, A. I. Frenkel and B. R. Cuenya, *J. Am. Chem. Soc.*, 2010, **132**, 15714-15719.
2. A. N. Shipway, E. Katz and I. Willner, *ChemPhysChem*, 2000, **1**, 18-52.
3. R. C. Jeff, Jr., M. Yun, B. Ramalingam, B. Lee, V. Misra, G. Triplett and S. Gangopadhyay, *Appl. Phys. Lett.*, 2011, **99**, 072104.
4. Z. Liu, M. Shamsuzzoha, E. T. Ada, W. M. Reichert and D. E. Nikles, *J. Power Sources*, 2007, **164**, 472-480.
5. C. Wang, H. Daimon, Y. Lee, J. Kim and S. Sun, *J. Am. Chem. Soc.*, 2007, **129**, 6974-6975.
6. K. Huang, H. Ma, J. Liu, S. Huo, A. Kumar, T. Wei, X. Zhang, S. Jin, Y. Gan, P. C. Wang, S. He, X. Zhang and X.-J. Liang, *ACS Nano*, 2012, **6**, 4483-4493.
7. F. d. r. Maillard, E. R. Savinova and U. Stimming, *J. Electroanal. Chem.*, 2007, **599**, 221-232.
8. J. Chen, B. Lim, E. P. Lee and Y. Xia, *Nano Today*, 2009, **4**, 81-95.
9. S. Mukherjee, B. Ramalingam, L. Griggs, S. Hamm, G. A. Baker, P. Fraundorf, S. Sengupta and S. Gangopadhyay, *Nanotechnology*, 2012, **23**, 485405.
10. M. Arenz, K. J. J. Mayrhofer, V. Stamenkovic, B. B. Blizanac, T. Tomoyuki, P. N. Ross and N. M. Markovic, *J. Am. Chem. Soc.*, 2005, **127**, 6819-6829.
11. S. Park, Y. Xie and M. J. Weaver, *Langmuir*, 2002, **18**, 5792-5798.

12. K. Yamamoto, T. Imaoka, W.-J. Chun, O. Enoki, H. Katoh, M. Takenaga and A. Sonoi, *Nat. Chem.*, 2009, **1**, 397-402.

13. S. Panigrahi, S. Basu, S. Praharaj, S. Pande, S. Jana, A. Pal, S. K. Ghosh and T. Pal, *J. Phys. Chem. C*, 2007, **111**, 4596-4605.

14. H. Song, R. M. Rioux, J. D. Hoefelmeyer, R. Komor, K. Niesz, M. Grass, P. Yang and G. A. Somorjai, *J. Am. Chem. Soc.*, 2006, **128**, 3027-3037.

15. J. Chen, T. Herricks and Y. Xia, *Angew. Chem.*, 2005, **117**, 2645-2648.

16. J. K. Navin, M. E. Grass, G. A. Somorjai and A. L. Marsh, *Anal. Chem.*, 2009, **81**, 6295-6299.

17. H. Patten, E. Ventosa, A. Colina, V. Ruiz, J. Lapez-Palacios, A. Wain, S. S. Lai, J. Macpherson and P. Unwin, *J. Solid State Electrochem.*, 2011, **15**, 2331-2339.

18. O. V. Cherstiouk, P. A. Simonov and E. R. Savinova, *Electrochim. Acta*, 2003, **48**, 3851-3860.

19. Y. Minseong, R. Balavinayagam and G. Shubhra, *Nanotechnology*, 2011, **22**, 465201.

20. S. Giuffrida, G. Ventimiglia, F. L. Callari and S. Sortino, *Eur. J. Inorg. Chem.*, 2006, 4022-4025.

21. S. Hrapovic, Y. Liu, K. B. Male and J. H. T. Luong, *Anal. Chem.*, 2003, **76**, 1083-1088.

22. M. H. Huang, Y. Shao, X. P. Sun, H. J. Chen, B. F. Liu and S. J. Dong, *Langmuir*, 2005, **21**, 323-329.

23. X. Yuan, N. Yan, C. Xiao, C. Li, Z. Fei, Z. Cai, Y. Kou and P. J. Dyson, *Green Chem.*, 2010, **12**, 228-233.

24. W. Tu, K. Takai, K.-i. Fukui, A. Miyazaki and T. Enoki, *J. Phys. Chem. B*, 2003, **107**, 10134-10140.

25. Y. Govender, T. L. Riddin, M. Gericke and C. G. Whiteley, *J. Nanopart. Res.*, 2010, **12**, 261-271.

26. J. Zeng, *J. Mater. Chem.*, 2012, **22**, 3170-3176.

27. B. H. San, S. Kim, S. H. Moh, H. Lee, D.-Y. Jung and K. K. Kim, *Angew. Chem. Int. Ed.*, 2011, **50**, 11924-11929.

28. R. Narayanan and M. A. El-Sayed, *J. Phys. Chem. B*, 2004, **108**, 5726-5733.

29. L. M. Forbes, A. M. Omahony, S. Sattayasamitsathit, J. Wang and J. N. Cha, *J. Mater. Chem.*, 2011, **21**, 15788-15792.

30. C.-Y. Lee, Y.-J. Choi and H.-H. Park, *J. Appl. Polym. Sci.*, **119**, 811-815.

31. J. A. Gilbert, N. N. Kariuki, R. Subbaraman, A. J. Kropf, M. C. Smith, E. F. Holby, D. Morgan and D. J. Myers, *J. Am. Chem. Soc.*, **134**, 14823-14833.

32. K. Esumi, R. Isono and T. Yoshimura, *Langmuir*, 2004, **20**, 237-243.

33. H. Ma, Y. Geng, Y.-I. Lee, J. Hao and H.-G. Liu, *Colloids Surf. A*, 2013, **419**, 201-208.

34. R. R. Bhattacharjee, M. Chakraborty and T. K. Mandal, *J. Nanosci. Nanotechnol.*, 2004, **4**, 844-848.

35. E. Dinda, M. H. Rashid, M. Biswas and T. K. Mandal, *Langmuir*, 2010, **26**, 17568-17580.

36. M. H. Rashid and T. K. Mandal, *J. Phys. Chem. C*, 2007, **111**, 16750-16760.

37. M. H. Rashid and T. K. Mandal, *Adv. Funct. Mater.*, 2008, **18**, 2261-2271.

38. N. Pradhan, A. Pal and T. Pal, *Langmuir*, 2001, **17**, 1800-1802.

39. T. Yu, J. Zeng, B. Lim and Y. Xia, *Adv. Mater.*, 2010, **22**, 5188-5192.

40. M. H. Rashid, M. Raula and T. K. Mandal, *J. Mater. Chem.*, 2011, **21**, 4904-4917.

41. S. Si, R. R. Bhattacharjee, A. Banerjee and T. K. Mandal, *Chem. Eur. J.*, 2006, **12**, 1256-1265.

42. R. R. Bhattacharjee, A. K. Das, D. Haldar, S. Si, A. Banerjee and T. K. Mandal, *J. Nanosci. Nanotechnol.*, 2005, **5**, 1141-1147.

43. Y. Li and Y. Huang, *Adv. Mater.*, 2010, **22**, 1921-1925.

44. Y. Li, G. P. Whyburn and Y. Huang, *J. Am. Chem. Soc.*, 2009, **131**, 15998-15999.

45. C. Lucio Colombi, M. Michael, S. Ralf, P. Wolfgang and V. Alessandro De, *Nanotechnology*, 2003, **14**, 840.

46. H. Zheng, R. K. Smith, Y.-w. Jun, C. Kisielowski, U. Dahmen and A. P. Alivisatos, *Science*, 2009, **324**, 1309-1312.

47. M. Raula, M. H. Rashid, S. Lai, M. Roy and T. K. Mandal, *ACS Appl. Mater. Interfaces*, 2012, **4**, 878-889.

48. M. Biswas, E. Dinda, M. H. Rashid and T. K. Mandal, *J. Colloid Interface Sci.*, 2012, **368**, 77-85.

49. S. Wunder, F. Polzer, Y. Lu, Y. Mei and M. Ballauff, *J. Phys. Chem. C*, **114**, 8814-8820.

50. B. Baruah, G. J. Gabriel, M. J. Akbashev and M. E. Booher, *Langmuir*, 2013, **29**, 4225-4234.

51. J. Zhang, G. Chen, M. Chaker, F. Rosei and D. Ma, *Appl. Catal., B*, 2013, **132-133**, 107-115.

52. M. H. Rashid, R. R. Bhattacharjee, A. Kotal and T. K. Mandal, *Langmuir*, 2006, **22**, 7141-7143.

53. R. Narayanan and M. A. El-Sayed, *Nano Lett.*, 2004, **4**, 1343-1348.

54. E. Hariprasad and T. P. Radhakrishnan, *Chem. Eur. J.*, 2010, **16**, 14378-14384.

55. K. Kuroda, T. Ishida and M. Haruta, *J. Molecular Catal. A: Chemical*, 2009, **298**, 7-11.

56. M. J. Beier, J.-M. Andanson and A. Baiker, *ACS Catalysis*, 2012, **2**, 2587-2595.

57. S. Ikeda, S. Ishino, T. Harada, N. Okamoto, T. Sakata, H. Mori, S. Kuwabata, T. Torimoto and M. Matsumura, *Angew. Chem. Int. Ed.*, 2006, **45**, 7063-7066.

Graphical contents entry

In Situ Synthesis of Ultra-small Platinum Nanoparticles Using Water Soluble Polyphenolic Polymer with High Catalytic Activity

Tanmoy Maji, Sanjib Banerjee, Mrinmoy Biswas and Tarun K. Mandal*

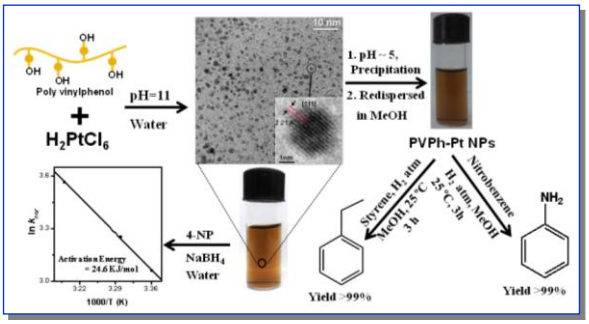

Ultra-small platinum nanoparticles are generated by *in situ* polymer reduction technique which shows high catalytic activity in water and in organic solvent.